

## Pressure and Temperature Evolution of the Structure of Solid $C_{70}$ .

C. CHRISTIDES, I. M. THOMAS, T. J. S. DENNIS and K. PRASSIDES

*School of Chemistry and Molecular Sciences, University of Sussex  
Brighton BN1 9QJ, UK*

(received 9 March 1993; accepted in final form 14 April 1993)

PACS. 61.12G - Neutron diffraction techniques (*e.g.* powder, single crystal, energy dispersive, and pulsed neutron source methods).

PACS. 64.70K - Solid-solid transitions.

PACS. 61.10F - Experimental techniques (*inc.* apparatus, techniques and calculation methods for analysing experimental results).

**Abstract.** - The pressure dependence of the structure of solid  $C_{70}$  at ambient temperature has been measured to 25 GPa by energy-dispersive X-ray diffraction. The face-centred cubic structure transforms irreversibly to a rhombohedral phase at 0.35 GPa. Crystalline  $C_{70}$  is stable to 18 GPa when a phase change to amorphous carbon occurs.  $C_{70}$  has a slightly smaller compressibility than  $C_{60}$ . The temperature dependence of the structure at ambient pressure has also been investigated by neutron diffraction. A transition to a rhombohedral phase occurs near 280 K with the f.c.c. structure coexisting at least to 200 K. The crystallographic symmetry of the lowest-temperature phase appears to be lower than rhombohedral. On warming, the rhombohedral phase is stable to 350 K. Strong static and dynamic disorder dominates the crystal chemistry of solid  $C_{70}$ .

**Introduction.** -  $C_{70}$  is the second most abundant fullerene present in the soluble extract from arc-processed carbon deposits [1, 2]. Its molecular structure is that of an ellipsoid (point group  $D_{5h}$ ) with five different types of carbon in the ratio 1:1:1:2:2 [2, 3]. In contrast to  $C_{60}$  for which a good understanding of its solid-state properties has already been developed [4-6], the structure and dynamics of solid  $C_{70}$  have not been fully elucidated. Early X-ray diffraction and electron microscopy studies [7, 8] have revealed that both cubic closed packed (c.c.p.) and hexagonal closed packed (h.c.p.) phases coexist, while a large concentration of defects is also present. Information on the molecular dynamics of c.c.p. solid  $C_{70}$  has come from both  $\mu$ SR [9, 10] and neutron scattering [11] studies: uniaxial rotation about the long molecular axis appears possible in the orientationally ordered phase even at  $\sim 100$  K, with re-orientational disorder setting in gradually at  $\sim 160$  K; anisotropy persists across the transition to an orientationally disordered phase in the vicinity of 270 K, with the molecular motion being essentially isotropic at 525 K. Temperature-dependent structural studies have only been performed on the minority h.c.p. structural modification [12-14] and reveal two phase transitions on cooling: first to a deformed h.c.p. structure followed by a transition to a monoclinic structure. Severe faults and substantial disorder present in the face-centred cubic

(f.c.c.) crystals have thus far precluded any detailed structural work on the majority c.c.p.  $C_{70}$  phase.

We have prepared a bulk  $C_{70}$  sample with a room temperature f.c.c. structure and undertaken a study of the pressure dependence of the crystal structure at ambient temperature using energy-dispersive X-ray diffraction. A f.c.c.  $\rightarrow$  rhombohedral ( $\alpha \sim 85.4(1)^\circ$ ) phase transition occurs at  $\sim 0.35$  GPa with no f.c.c. phase present above  $\sim 1.0$  GPa. A transition to an amorphous carbon phase occurs gradually above  $\sim 11$  GPa with no crystalline  $C_{70}$  evident at  $> 18$  GPa. We have also performed a powder neutron diffraction study of the temperature dependence of the crystal structure of  $C_{70}$ . On cooling, we find a phase transition at  $\sim 280$  K to the same rhombohedral phase ( $\alpha \sim 85.6(1)^\circ$ ), again consistent with molecular alignment along the [111] crystalline direction. The phase coexistence region extends at least down to  $\sim 200$  K. Below this temperature, the profile remains unchanged and is consistent with a crystallographic phase of lower symmetry than rhombohedral. On heating, the rhombohedral phase persists past the transition temperature to temperatures as high as  $\sim 340$  K.

*Experimental.* – The  $C_{70}$  powder was separated from  $C_{60}$  by alumina column chromatography using hexane as eluent. After washing with acetone, the solid extract was recrystallised from benzene. It was then sublimed at 840 K using a small cylindrical furnace, placed in a bell-jar high-vacuum system ( $10^{-6}$  Torr). In all, 500 mg of sublimed  $C_{70}$  crystalline powder were produced in this way ( $\geq 98.5\%$   $C_{70}$ ,  $\leq 1.5\%$   $C_{60}$ ). The final treatment of the sample involved extended annealing at 250  $^\circ$ C ( $\geq 2$  days) in sealed quartz tubes. The  $C_{70}$  purity was established with infra-red and  $^{13}$ C NMR spectroscopy and X-ray powder diffraction (Siemens D5000). Prompt  $\gamma$ -ray neutron activation analysis [15] at the National Institute of Standards and Technology, Gaithersburg (USA) gave a total hydrogen content of 0.046(7)% by weight, i.e. roughly one H atom for every three  $C_{70}$  molecules.

The high-pressure energy-dispersive X-ray diffraction experiments at ambient temperature were performed on Station 9.7 at the Synchrotron Radiation Source (SRS), Daresbury Laboratory (UK). Small samples of  $C_{70}$  powder ( $(0.3 \div 1.0)$  mg) were loaded in INCONEL gaskets along with a pressure calibrant (NaCl powder) and a hydrostatic-pressure medium (methanol/ethanol (4:1) mixture) in diamond anvil pressure cells. Pressures as high as 25 GPa were attained. Employing an incident angle of  $2\theta = 5.781^\circ$  over the energy range (10  $\div$  50) keV allowed the separation of the  $C_{70}$  diffraction peaks from those arising from the gasket. Neutron diffraction profiles were recorded between 5 and 470 K on the high-resolution powder diffractometer (HRPD) at the ISIS Facility, Rutherford Appleton Laboratory (UK) with the sample at the low-resolution high-flux position over a time-of-flight range (30  $\div$  230) ms. The sample was placed either inside a cylindrical ( $(5 \div 340)$  K) or a flat-window ( $(340 \div 470)$  K) vanadium can in a continuous-flow helium cryostat. Remarkably the measured diffraction profiles in backscattering mode ( $\Delta d/d = 8 \cdot 10^{-4}$ ), covering a  $d$ -spacing range of  $(0.6 \div 3.2)$  Å, showed virtually no Bragg peaks present. Consequently only data collected with the  $90^\circ$  detector bank ( $\Delta d/d = 2 \cdot 10^{-3}$ ) which allowed access up to 5.7 Å in  $d$ -spacing were used.

*Results and discussion.* – In fig. 1 we show typical laboratory X-ray diffraction (XRD) profiles of two sublimed  $C_{70}$  samples. Sample B is not single phase and the peaks may be indexed assuming the presence of both a f.c.c. ( $a = 14.943(1)$  Å) and a rhombohedral ( $a = 14.96(2)$  Å,  $\alpha = 85.7(1)^\circ$ ) phase. Sample A has been vacuum annealed and is essentially a pure f.c.c. ( $a = 14.898(6)$  Å) phase. The sawtooth low-angle shoulder of the (111) peak is indicative of the presence of stacking faults, reminiscent of the situation encountered in  $C_{60}$ . In general, the proportion of rhombohedral contamination of the as-sublimed material was found to vary randomly among different batches.

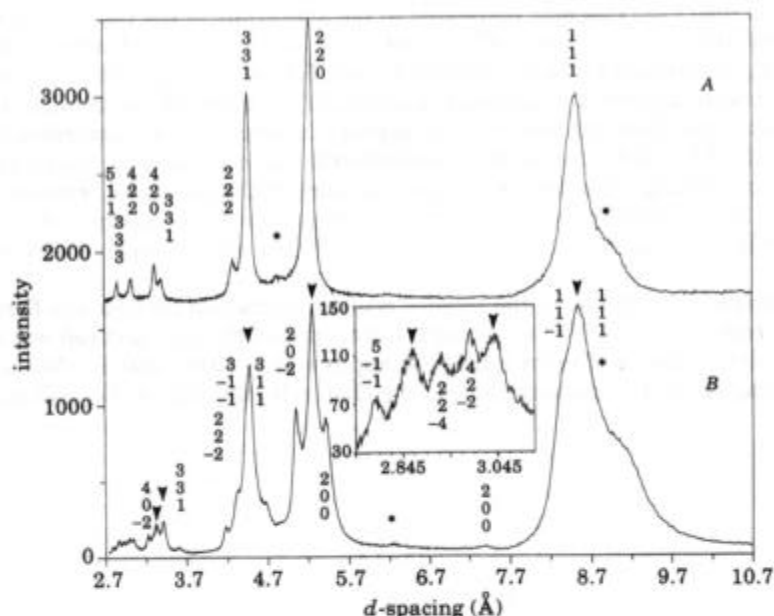


Fig. 1. - X-ray diffraction profiles of  $C_{70}$  measured at room temperature using  $CuK\alpha$  radiation.  $B$  is a mixture of a f.c.c. and a rhombohedral phase for the as-sublimed solid.  $A$  is the f.c.c. phase derived after vacuum annealing of  $B$ . Indexing of the peaks refers to the rhombohedral phase, the arrows denote the f.c.c. peak positions and the (\*) marks peaks arising from the presence of stacking faults.

Figure 2 shows some characteristic energy-dispersive XRD patterns observed in the high-pressure ambient temperature measurements. At 0.1 GPa (1 GPa = 10 kbar), the structure is f.c.c. with a lattice constant  $a = 14.939(6)$  Å. The low-energy peak arising from the large concentration of stacking faults is again clearly visible. When a pressure of 0.35 GPa (fig. 2b)) is reached, a second phase appears, characterised by the splitting of the f.c.c. 111, 220 and 311 peaks, and coexists with the f.c.c. phase. The new phase could be indexed using a rhombohedral unit cell. When a pressure of 1 GPa is reached, no f.c.c. fraction remains. The f.c.c.  $\rightarrow$  rhombohedral phase transition is irreversible and, upon release of the pressure,  $C_{70}$  is found in the rhombohedral phase. The change in the lattice parameters observed as a function of pressure is shown in the inset of fig. 3; a monotonic decrease in  $a$  is observed for both the f.c.c. and rhombohedral phases, while the rhombohedral angle  $\alpha$  does not significantly change with increasing pressure, implying that the molecular orientation with respect to the  $\langle 111 \rangle$  crystalline direction changes little (average =  $85.4(1)^\circ$ ). Our present observations are consistent with an earlier report of the presence of a rhombohedral phase above 1.2 GPa [16].

Only four data points were obtained for the f.c.c. phase of  $C_{70}$ , making the equation of state (EOS) for this phase impossible to calculate with any accuracy. The pressure-volume curve for the rhombohedral phase up to 6 GPa is shown in fig. 3. The data were fitted well (solid line) using the Murnaghan EOS [17]:  $P = (K_0/K'_0)[(V_0/V)^{K'_0} - 1]$ , where  $K_0$  is the bulk modulus,  $K'_0$  is its pressure derivative ( $= dK_0/dP$ ), and  $V_0$  is the unit cell volume at zero pressure.  $K_0$  was found to be 25(9) GPa (compressibility  $\kappa = (4.0 \pm 4) \cdot 10^{-2} \text{ GPa}^{-1}$ ) as compared to 18.1(1.8) GPa for the simple cubic phase of  $C_{60}$  [18], making  $C_{70}$  a little less

compressible than  $C_{60}$ . This may be related to the anisotropy of the  $C_{70}$  molecules compared to the quasi-spherical  $C_{60}$  units which can pack much more efficiently. The pressure derivative  $K'_0$  is 10.6(1.3) for rhombohedral  $C_{70}$  (cf. 5.7(0.6) for  $C_{60}$ ). When pressures higher than 6.5 GPa were applied, a progressive reduction of the intensities of the  $311$ ,  $3\bar{1}\bar{1}$ ,  $11\bar{3}$ , and  $22\bar{2}$  reflections was observed and the solid appears to become more compressible. This may be associated with a distortion of the rhombohedral unit cell, possibly driven by a reduced shear strength arising from the anisotropic structure of the molecules. Further increase of pressure to 11 GPa results in the irreversible appearance of an amorphous carbon phase; complete collapse of the Bragg intensity occurs by 18 GPa with amorphous carbon present to 25 GPa.

The temperature evolution of the powder neutron diffraction profiles was first monitored by cooling from 340 to 5 K. No low-symmetry distortion of the f.c.c. unit cell was apparent at 340 K. The first evidence of extra reflections appears at  $\sim (300 \div 280)$  K when a small peak starts growing on the low  $d$ -spacing side of the (220) reflection (fig. 4). On cooling, new peaks

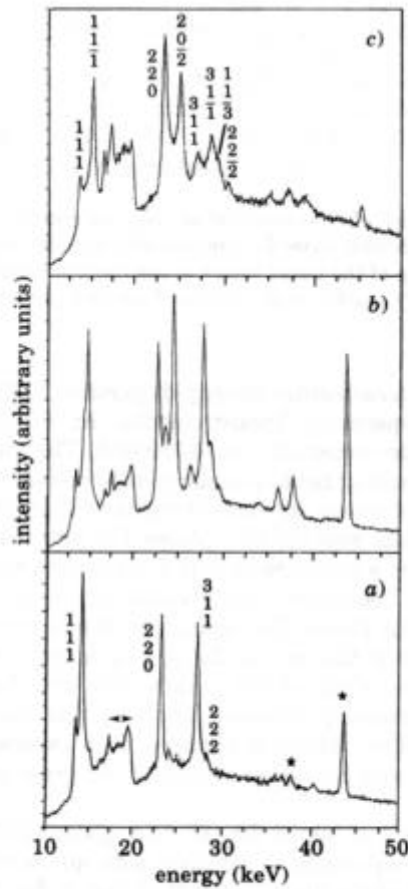


Fig. 2. - Energy dispersive X-ray diffraction patterns of pressurised  $C_{70}$  at ambient temperature (incident angle,  $2\theta = 5.781^\circ$ ). a) Ambient pressure. b)  $P = 0.35$  GPa. c)  $P = 1.0$  GPa. The area marked by ( $\leftarrow \rightarrow$ ) relates to reflections from the INCONEL gasket. \* marks the NaCl pressure calibrant reflections.

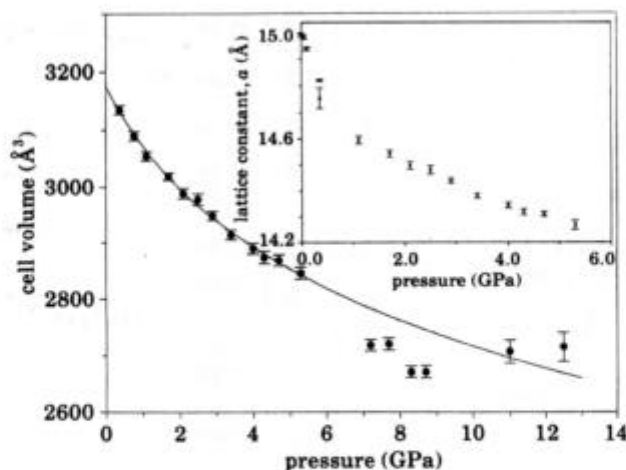


Fig. 3. - Pressure-volume plot for rhombohedral  $C_{70}$ . The solid line is a fit to the Murnaghan EOS with  $K_0 = 25(9)$  GPa and  $K'_0 = 10.6(1.3)$ ,  $V_0 = 3175(10) \text{ \AA}^3$ . Inset: pressure dependence of the lattice constant.

grow at the expense of the f.c.c. reflections. The diffraction profile develops gradually down to 200 K. Little change occurs below this temperature down to 5 K. In agreement with the pressure results, the observed diffraction profiles in the  $(280 \pm 200)$  K temperature range can be rationalised by considering the co-existence of a f.c.c. and a rhombohedral phase. What appears remarkable is that a fraction of the high-symmetry disordered phase persists to very low temperatures. Below 200 K, the diffraction profile is consistent with the existence of an orientationally ordered structure with symmetry lower than rhombohedral; since orthorhombic crystallographic symmetry will be incompatible with c.c.p. and the  $C_{70}$  molecular symmetry, the low-temperature structure is very likely monoclinic.

We also followed the temperature evolution of the diffraction profiles by heating from 5 to 470 K. The rhombohedral  $\rightarrow$  f.c.c. phase transition occurs fairly abruptly upon heating at  $\sim 270$  K. However, the transformation is not complete, resulting in a diminishing fraction of the rhombohedral phase being present up to 340 K. The phase change thus appears to be very sluggish, showing both undercooling and overheating effects. Presumably the concentration of defects and stacking faults arising from both structural (static) and orientational (dynamic) disorder is so large that the low-symmetry structure is pinned down and excess thermal energy is needed to overcome the energy barriers arising from structural imperfections. No detectable change in the profiles occurs to 470 K with the widths of the observed f.c.c. reflections showing no broadening above 300 K, that would indicate any further phase changes in this temperature range.

The temperature dependence of the structural results is shown in fig. 5. Consistent with earlier studies of the dynamic properties of  $C_{70}$  [9-11], the structure is f.c.c. at high temperatures in agreement with the quasi-isotropic motion of the ellipsoidal molecules. The appearance of the rhombohedral phase on cooling (or on the application of pressure) is a result of molecular orientational ordering; the data of fig. 5 are consistent with the molecules preferentially orienting along the unit cell diagonal. This is reflected in both an abrupt expansion along  $\langle 111 \rangle$  (fig. 5a)) as the long axis of the molecules is now pointing towards this direction and an abrupt contraction along the close-packing  $\langle 110 \rangle$  direction (fig. 5b)) reflecting their smaller size on the equatorial plane. A small volume change (fig. 5c)) is also

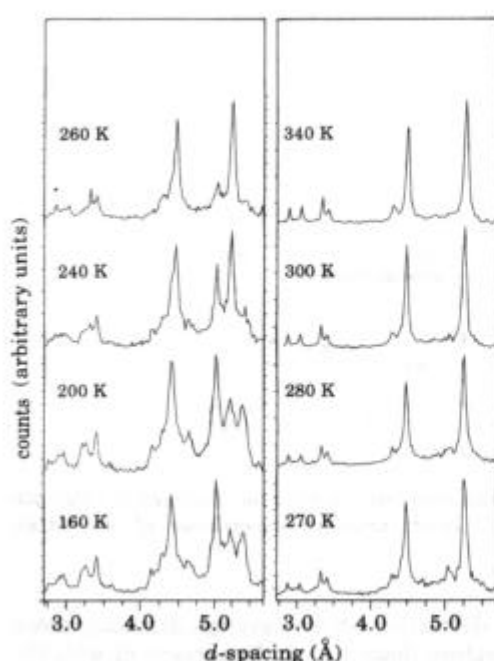


Fig. 4

Fig. 4. - Powder neutron diffraction profiles of  $C_{70}$  recorded between 340 and 160 K (cooling) showing the progressive appearance of the low-temperature phases.

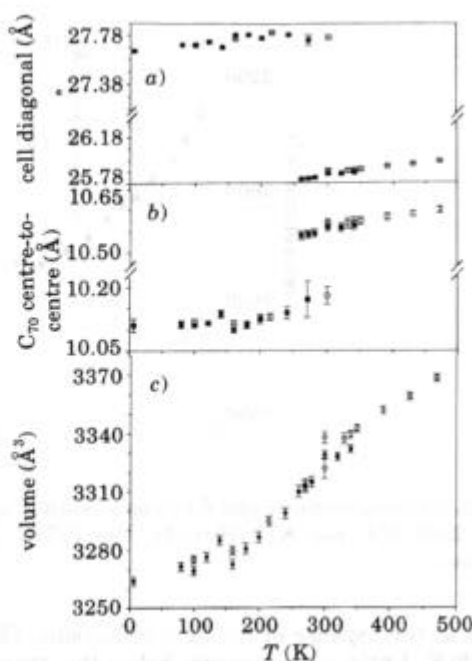


Fig. 5

Fig. 5. - Temperature evolution of the unit cell dimensions in solid  $C_{70}$ . a) Unit cell diagonal ( $\langle 111 \rangle$  direction). b)  $C_{70}$  centre-to-centre distance on the close-packing (110) plane. c) Unit cell volume. A pseudo-rhombohedral unit cell was used for the low-temperature phases. Open symbols refer to data collected during a warming-up cycle and filled symbols to a cooling-down cycle. (○) label the rhombohedral and (□) the f.c.c. phase.

observed at the phase transition, while the rhombohedral angle  $\alpha$  does not change with temperature.

Molecular-dynamics calculations of f.c.c.  $C_{70}$  [19] predict the presence of two phase transitions (f.c.c.  $\rightarrow$  rhombohedral  $\rightarrow$  monoclinic) on cooling. The rhombohedral phase results from the ordering of the  $C_{70}$  long axis towards the  $\langle 111 \rangle$  direction, while the molecules themselves remain disordered. No change in lattice dimensions is calculated to occur at  $T_c$ , with the rhombohedral angle being  $\sim 86^\circ$ . These predictions are in excellent agreement with our experimental data. However, the presence of substantial disorder in the sample does not make it possible to present definite conclusions on the lower-symmetry phases. A puzzling feature also relates to the reports from experimental measurements of the thermal properties [8,20] of solid  $C_{70}$  that a phase transition also occurs in the vicinity of 350 K. We checked meticulously our diffraction profiles in this temperature range and we find no evidence of any changes occurring. However, it is tempting to note that it is precisely at this temperature that, on heating, the «overheated» rhombohedral phase is finally converted to the f.c.c. phase, as the hindrance potential barrier associated with microstrains and defects appears to be of the order of 350 K.



**Conclusion.** – In conclusion, we find that solid  $C_{70}$  adopts a f.c.c. crystal structure at high temperature. A rhombohedral distortion ( $\alpha \sim 85.6(1)^\circ$ ) accompanies an orientational ordering transition as the molecules orient themselves towards the unit cell diagonal; however, they still appear to spin about their long axis, which also performs a tumbling type of motion. The f.c.c. and rhombohedral phases coexist over a large temperature range. A lower-symmetry crystallographic phase (possibly monoclinic [19]) is present below 200 K. Modest pressure is also enough to cause an ordering transition irreversibly, the resulting rhombohedral structure being slightly more compressible than  $C_{60}$ . Large hydrostatic pressures ( $> 11$  GPa) lead to the formation of an amorphous carbon phase. The structural properties of  $C_{70}$  are also found to be dominated by a high concentration of defects, associated with static and dynamic disorder, that lead to extensive «undercooling» for the f.c.c. phase and «overheating» behaviour for the rhombohedral phase.

*Additional Remark.*

In a recent preprint, Vaughan *et al.*, [21] reported a high-resolution X-ray powder diffraction study of solid  $C_{70}$ . They found that the low-temperature phase is indeed monoclinic with the ABC packing retained at all temperatures. Disorder effects are also discussed in detail.

\*\*\*

We thank the Science and Engineering Research Council, UK, for financial support and the Rutherford Appleton Laboratory and Daresbury Laboratory for provision of beam time. We also acknowledge the invaluable help of S. J. CLARK and R. M. IBBERTSON with the experiments.

## REFERENCES

- [1] KRÄTSCHMER W., LAMB L. D., FOSTIROPOULOS K. and HUFFMAN D. R., *Nature*, **347** (1990) 354.
- [2] TAYLOR R., HARE J. P., ABDUL-SADA A. and KROTO H. W., *J. Chem. Soc. Chem. Commun.*, (1990) 1423.
- [3] KROTO H. W., *Science*, **242** (1988) 1139.
- [4] PRASSIDES K., KROTO H. W., TAYLOR R., WALTON D. R. M., DAVID W. I. F., TOMKINSON J., ROSSEINSKY M. J., MURPHY D. W. and HADDON R. C., *Carbon*, **30** (1992) 1277.
- [5] HEINEY P. A., *J. Phys. Chem. Solids*, **53** (1992) 1333.
- [6] COPLEY J. R. D., NEUMANN D. A., CAPPELLETTI R. L. and KAMITAKAHARA W. A., *J. Phys. Chem. Solids*, **53** (1992) 1353.
- [7] VAN TENDELOO G. *et al.*, *Europhys. Lett.*, **15** (1991) 295.
- [8] VAUGHAN G. B. M., HEINEY P. A., FISCHER J. E., LUZZI D. E., RICKETTS-FOOT D. A., MCGHIE A. R., HUI Y.-W., SMITH A. L., COX D. E., ROMANOW W. J., ALLEN B. H., COUSTEL N., MCCAULEY J. P. and SMITH A. B., *Science*, **254** (1992) 1350.
- [9] PRASSIDES K., DENNIS T. J. S., CHRISTIDES C., RODUNER E., KROTO H. W., TAYLOR R. and WALTON D. R. M., *J. Phys. Chem.*, **96** (1992) 10600.
- [10] DENNIS T. J. S., PRASSIDES K., RODUNER E., CRISTOFOLINI L. and DE RENZE R., submitted to *J. Phys. Chem.*.
- [11] CHRISTIDES C., DENNIS T. J. S., PRASSIDES K., CAPPELLETTI R. L., NEUMANN D. A. and COPLEY J. R. D., submitted to *Phys. Rev. B*.
- [12] VERHELJEN M. A., MEEKES H., MELJER G., BENNEMA P., DE BOER J. L., VAN SMAALEN S., VAN TENDELOO G., AMELINCKX S., MUTO S. and VAN LANDUYT J., *Chem. Phys.*, **166** (1992) 287.

- [13] VAN TENDELOO G., AMELINCKX S., DE BOER J. L., VAN SMAALEN S., VERHEIJEN M. A., MEEKES H. and MEIJER G., *Europhys. Lett.*, **21** (1993) 329.
- [14] GREEN M. A., KURMOO M., DAY P. and KIKUCHI K., *J. Chem. Soc. Chem. Commun.*, (1992) 1676.
- [15] FAILEY M. P., ANDERSON D. L., ZOLLER W. H., GORDON G. E. and LINDSTROM R. M., *Anal. Chem.*, **51** (1979) 2209.
- [16] KAWAMURA H., KOBAYASHI M., AKAHAMA Y., SHINOHARA H., SATE H. and SAITO Y., *Solid State Commun.*, **83** (1992) 563.
- [17] MURNAGHAN F. D., *Proc. Natl. Acad. Sci.*, **30** (1947) 244.
- [18] DUCLOS S. J., BRISTER K., HADDON R. C., KORTAN A. R. and THIEL F. A., *Nature*, **351** (1991) 380.
- [19] SPRIK M., CHENG A. and KLEIN M. L., *Phys. Rev. Lett.*, **69** (1992) 1660.
- [20] GRIVEI E., NYSTEN B., CASSART M., ISSI J. P., FABRE C. and RASSAT A., *Phys. Rev. B*, **47** (1993) 1705.
- [21] VAUGHAN G. B. M., HEINEY P. A., COX D. E., FISCHER J. E., MCGHIE A. R., SMITH A. L., STRONGIN R. M., CICHY M. A. and SMITH A. B., to be published.